

Article

Perhalophenyl–Phosphide: A Couple Needed to Stabilize Phosphide–Gold Complexes

Laura Coconubo-Guio , María Rodríguez-Castillo, Sonia Moreno, Miguel Monge , M. Elena Olmos * and José M. López-de-Luzuriaga *

Departamento de Química, Instituto de Investigación en Química (IQUR), Complejo Científico Tecnológico, Universidad de La Rioja, Madre de Dios 53, 26006 Logroño, Spain; laura-carolina.coconubo@unirioja.es (L.C.-G.); maria.rodriguez@unirioja.es (M.R.-C.); miguel.monge@unirioja.es (M.M.)

* Correspondence: m-elena.olmos@unirioja.es (M.E.O.); josemaria.lopez@unirioja.es (J.M.L.-d.-L.)

Abstract: The synthesis of gold(III) and gold(I)–gold(III) complexes with phosphide bridges is still a matter that requires solutions for their marked instability, in spite of the affinity of this metal in both oxidation states for phosphorous donor ligands. In the course of our studies, we realized that the presence of perhalophenyl groups of the type pentafluorophenyl or 3,5-dichlorotrifluorophenyl in the complexes gives rise to an increase in their stability that eases their isolation and structural characterization. In this paper, we describe two new fully characterized neutral compounds of this type to extend the knowledge on this family of compounds, $[\{\text{Au}(\text{C}_6\text{Cl}_2\text{F}_3)_2\}_2(\mu\text{-PPh}_2)_2]$ (1) and $[\{\text{Au}(\text{C}_6\text{Cl}_2\text{F}_3)_2(\mu\text{-PPh}_2)_2\text{Au}\}_2]$ (2). In this work, we analyze the role of the perhalophenyl groups in the stability of these complexes by using quantum chemical topology methodologies, specifically employing an analysis of the non-covalent interactions (NCIs) in real space and evaluating the electrostatic potential surfaces (ESP). Our findings reveal the existence of appreciable π -stacking interactions among the perhalophenyl and phenyl groups in both compounds, significantly contributing to the stability of the systems.

Keywords: gold(I); gold(III); phosphides; computational studies



Citation: Coconubo-Guio, L.;

Rodríguez-Castillo, M.; Moreno, S.;

Monge, M.; Olmos, M.E.;

López-de-Luzuriaga, J.M.

Perhalophenyl–Phosphide: A Couple Needed to Stabilize Phosphide–Gold Complexes. *Inorganics* **2024**, *12*, 78.

<https://doi.org/10.3390/inorganics12030078>

Academic Editor: Jean Pierre Djukic

Received: 31 January 2024

Revised: 27 February 2024

Accepted: 1 March 2024

Published: 3 March 2024



Copyright: © 2024 by the authors. Licensee MDPI, Basel, Switzerland. This article is an open access article distributed under the terms and conditions of the Creative Commons Attribution (CC BY) license (<https://creativecommons.org/licenses/by/4.0/>).

1. Introduction

Gold, in its more stable oxidation states (+1 and +3), has an enormous affinity for group five-element donor ligands, specifically tertiary phosphines. Nevertheless, bonds between gold(I) or gold(II) and donor atoms of amines, arsines or stibines are also known, although they are less common than those with phosphorus atoms of phosphines.

In contrast, in the case of non-tertiary phosphines, the number of examples of gold complexes decreases considerably, a fact that could presumably be attributed to the relatively lower stability of these ligands compared with the former. The number of examples arising from the deprotonation of secondary or primary phosphines, those called phosphides, is also very scarce, especially in the case of gold(III) [1–9]. In fact, nowadays, this is still a pending subject that requires much more work because polynuclear phosphide complexes are expected to show catalytic activity, and because the strong donor and bridging abilities of PR_2^- groups can facilitate the proximity of gold centers at short distances, in turn facilitating the optical or sensing properties associated with this effect [10].

Our research group has contributed numerous examples of this type of complex, starting from secondary phosphines and perhalophenyl gold(III) precursors [5–7]. This still limited knowledge has allowed us to presume that the halogenated aromatic ligands that accompany gold(III) might have a very important role in the stabilization of the phosphide derivatives, since other anionic ligands, such as halogens, give rise to decomposition or non-desired products [11]. Thus, the extensive use of perhalophenyl groups as accompanying ligands has led us to establish it as a general strategy for the preparation of new phosphide complexes.

In the beginning of our research on this topic, at the end of the last century and in the beginning of the present one, the sole perhalophenyl group used in the synthesis of this type of complex was pentafluorophenyl (C_6F_5) [5,6]. Recently, we resumed this topic and we reported the synthesis of two new mixed gold(III)–gold(I) phosphide complexes following the so-called “*acac* method” synthetic procedure [7], and in which the perhalophenyl group used to stabilize the complexes was the poorly represented 3,5-dichlorotrifluorophenyl ligand. Our interest, in that case, was in checking how the different substituents in the aryl groups (in terms of electronegativity and steric demand) could affect the stability of the synthesized complexes. Nevertheless, we did not detect significant differences with those previously described compounds. Therefore, the question remains: How do perhalophenyl groups influence the stability of the phosphide gold complexes?

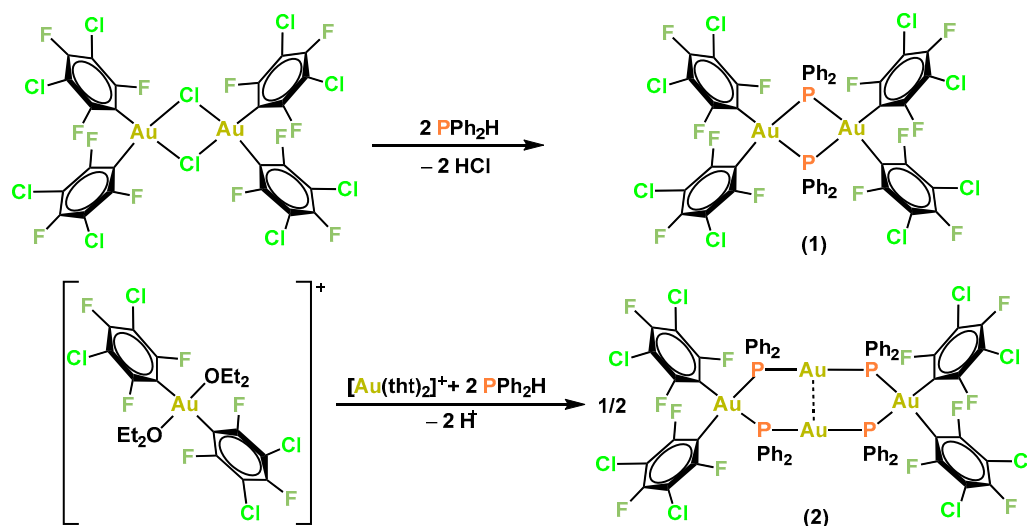
To answer this question, we prepared two new neutral organometallic cyclic complexes with phosphide bridges of gold. The first one is a four-membered cyclic compound with two gold(III) centers doubly bridged by two diphenylphosphide ligands, while the second one corresponds to a tetranuclear eight-membered ring with mixed-valence metallic centers (Au^{III}/Au^I) and PPh_2^- groups bridging them. This study has allowed us to analyze the stability of the complexes when varying the oxidation states of gold. On the other hand, we have different model systems that permit us to theoretically analyze the electronics of these complexes by means of a NCI and ESP topological analysis of the DFT-computed densities, and how the presence of perhalophenyl groups could be essential in their stability.

2. Results and Discussion

2.1. Synthesis and Characterization of the Complexes

2.1.1. Synthesis and Spectroscopic Characterization

The synthesis of these two new compounds, summarized in Scheme 1, was carried out employing two different gold(III) precursors and synthetic routes. Thus, the doubly bridged dimeric gold(III) phosphide complex $[[Au(C_6Cl_2F_3)_2]_2(\mu-PPh_2)_2]$ (**1**) was prepared through the treatment of the chloro-bridged dinuclear gold(III) complex $[Au_2(C_6Cl_2F_3)_4(\mu-Cl)_2]$ in Et_2O with diphenylphosphine in a 1:2 molar ratio (see Scheme 1). In this process, the chlorine atoms serve as deprotonating agents, leading to the formation of the diphenylphosphide ligands, which act as bridges in the novel dinuclear compound **1**, with the subsequent elimination of two molecules of HCl per molecule of compound.



Scheme 1. Synthesis of complexes **1** and **2**.

Complex **1** is isolated as a white solid in a moderate yield. It exhibits a moderate stability in the presence of air and moisture and is soluble in chlorinated solvents and acetone, while demonstrating insolubility in diethyl ether and *n*-hexane. In acetone solution, it displays non-conducting behavior, in accordance with its neutral nature. Its

analytical and spectroscopic data corroborate the proposed stoichiometry. For instance, its infrared (IR) spectrum shows the characteristic absorptions attributable to the $C_6Cl_2F_3^-$ ligands bonded to the gold(III) centers, which appear at 1593 (vs), 1055 (vs), 1136 (vs) and 779 cm^{-1} (vs). Moreover, its HR-MS spectrum, acquired in negative mode, displays a peak at $m/z = 1594.7359$ Da, corresponding to the anionic fragment $[M + Cl]^-$, and confirming the exact molecular weight of the new complex **1**. In addition, this peak displays an experimental isotope pattern in accordance with the simulated one for the fragment $[M + Cl]^-$. On the other hand, the 1H NMR spectrum of compound **1** only shows resonances due to aromatic protons, confirming the presence of the Ph groups and the deprotonation of the diphenylphosphine ligand. This last fact is corroborated by the absence in this spectrum of the resonance attributed to the *H-P* atom, which appears at $\delta = 6.18$ ppm in the related diphenylphosphine derivative $[Au(3,5-C_6Cl_2F_3)_3(PPh_2H)]$ [7]. Regarding its ^{19}F NMR spectrum, it displays two singlets (with a relative integration of 2:1) at $\delta = -94.55$ and -114.27 ppm, which correspond to the fluorine atoms in the relative *ortho* and *para* positions, respectively, in the aryl groups present in the novel compound **1**.

Finally, the $^{31}P\{^1H\}$ NMR spectrum of **1** exhibits a unique resonance, which appears as a broad singlet at $\delta = -137.0$ ppm, and which is assigned to the two equivalent phosphorus atoms of the phosphide ligands, and the broadening of the resonance is probably caused by the coupling of these phosphorus atoms with the *ortho* fluorine nuclei of the perhalophenyl groups. This highly negative chemical shift closely resembles those observed in the isoelectronic Pt(II)-phosphide systems showing a Pt_2P_2 four-membered ring [12,13].

On the other hand, the tetranuclear $Au^{III}-Au^I$ complex $[Au(C_6Cl_2F_3)_2(\mu-PPh_2)_2Au]_2$ (**2**) was synthesized through the treatment of a freshly prepared solution of $[Au(C_6Cl_2F_3)_2(OEt)_2](ClO_4)$, which is obtained from the reaction of the precursor anionic gold(III) complex $NBu_4[Au(C_6Cl_2F_3)_2Cl_2]$ with $AgClO_4$ in diethyl ether, with the gold(I) cationic complex $[Au(tht)_2]ClO_4$ (tht = tetrahydrothiophene) and diphenylphosphine in a 1:1:2 molar ratio, as depicted in Scheme 1. Complex **2** is isolated as a white solid in good yield, exhibiting stability in the presence of air and moisture, and showing similar solubilities to those commented above for complex **1**. It is non-conducting in acetone solution and its analytical and spectroscopic data are consistent with the postulated stoichiometry and disposition of ligands. Hence, its IR spectrum exhibits similar absorptions to those observed for **1**, which are assigned to the $C_6Cl_2F_3$ groups coordinated to gold(III). Regarding its HR-MS spectrum, acquired in positive mode, it shows a peak at $m/z = 2346.8008$ Da, which corresponds to the cationic fragment $[M + Na]^+$, confirming the exact molecular weight of **2**. In addition, this peak displays an experimental isotope pattern in accordance with the simulated one for the fragment $[M + Na]^+$. On the other hand, the 1H NMR spectrum of the new complex **2**, as in the case of **1**, only reveals resonances attributed to aromatic protons, which also confirms the deprotonation of the secondary phosphine ligands. Furthermore, the ^{19}F NMR spectrum of **2** closely resembles that of compound **1**, displaying the same pattern with resonances due to the fluorine atoms in relative *ortho* and *para* positions in the aryl groups, just showing a very small shift of the resonances (see the Section 3). Finally, the most significant difference between these two compounds is found in their $^{31}P\{^1H\}$ NMR spectra. Specifically, the $^{31}P\{^1H\}$ NMR spectrum of compound **2** shows a singlet that appears shifted to a much more down-field chemical shift ($\delta = 35.6$ ppm) when compared to that of compound **1** ($\delta = -137.0$ ppm). This shift is probably due to the effect of the presence of more electron-rich gold(I) atoms, as well as to the different dimensionality of the heterocyclic ring in both complexes.

It is worth mentioning that these experimental data presented for the novel derivatives **1** and **2** are quite similar to those previously reported for the related pentafluorophenyl phosphide complexes $[Au_2(C_6F_5)_4(\mu-PPh_2)_2]$ [6] and $[Au(C_6F_5)_2(\mu-PPh_2)_2Au]_2$ [5], as previously described by our research group, thereby corroborating the proposed stoichiometries.

2.1.2. Crystal Structures

Single crystals of complexes **1** and **2** suitable for X-ray diffraction studies were acquired through the slow evaporation of chloroform or diethylether solutions of the complexes, respectively. Complex **1** crystallizes in the $P2_1/n$ space group within the monoclinic system with 0.75 molecules of solvent (chloroform) per molecule of metallic complex. The structure of $1 \cdot 0.75\text{CHCl}_3$ (Figure 1) shows a doubly bridged dimeric gold(III) phosphide compound in which the gold(II) centers display a distorted square-planar geometry imposed by the rigidity of the four-membered heterocycle, thus displaying P-Au-P angles smaller than expected ($79.69(4)$ and $79.51(4)^\circ$), while the C-Au-P ones are, on the contrary, greater than those corresponding to this geometry (ranging from $93.83(13)$ to $96.97(14)^\circ$). For the same reason, the tetrahedral environment of the bridging phosphorus atoms of the diphenylphosphide ligands is also distorted, and, thus, the Au-P-Au angles display values of $100.36(4)$ and $100.37(4)^\circ$, which are smaller than expected. Another effect of the formation of the four-membered cycle is the proximity of the gold centers, which are located at a distance of $3.6273(3)$ Å. Although this distance could be indicative of the presence of a weak aurophilic interaction, since it is shorter than twice the van der Waals radius of gold [14,15], the computational studies carried out on a model system based in this crystal structure (see below) demonstrate that this proximity is just forced by the bridging ligands and does not imply any degree of metal-metal bonding. Regarding the Au-C ($2.068(5)$ – $2.080(4)$ Å) and Au-P bond lengths ($2.357(1)$ – $2.366(1)$ Å), they display typical values for gold(III) complexes. In particular, if we compare this molecular structure with that of the pentafluorophenyl phosphide derivative $[\text{Au}_2(\text{C}_6\text{F}_5)_4(\mu\text{-PPH}_2)_2]$ [6], which shows the same structural arrangement, we find similar $\text{Au}^{\text{III}}\text{-C}$ bond distances of $2.055(7)$ and $2.060(8)$ Å, and nearly identical $\text{Au}^{\text{III}}\text{-P}$ bond lengths of $2.362(2)$ and $2.365(2)$ Å.

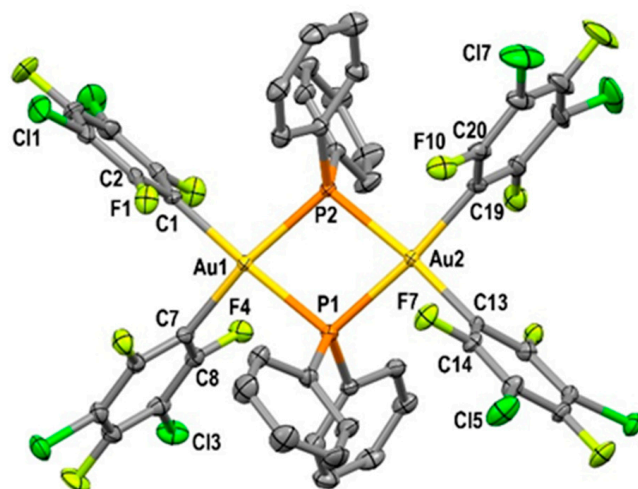


Figure 1. Molecular structure of $1 \cdot 0.75\text{CHCl}_3$ with the labelling scheme for the atom positions. Hydrogen atoms and solvent have been omitted for clarity. Selected bond lengths [Å] and angles [$^\circ$]: Au-P: $2.357(1)$ – $2.366(1)$, Au-C: $2.068(5)$ – $2.080(4)$, P-Au-P: $79.51(4)$ and $79.69(4)$, C-Au-C: $89.8(2)$ and $90.7(2)$, Au-P-Au: $100.36(4)$ and $100.37(4)$.

In the case of complex **2**, unfortunately, the low quality of the crystals precludes the determination of bond lengths and angles with sufficient accuracy, although a rough description of its structure can be done. As can be seen in Figure 2, the structure of the tetranuclear mixed valence gold complex **2** consists of an eight-membered ring in a twisted chair conformation that displays alternating gold and phosphorus atoms. The gold(I) centers maintain an intramolecular aurophilic interaction of about 2.95 Å, presumably responsible for the weak distortion of the linear environment of the monovalent gold atoms, while the gold(III) centers display a regular square-planar geometry.

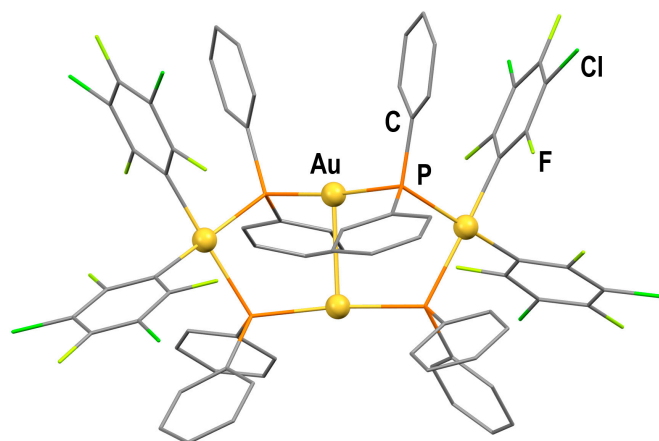


Figure 2. Molecular structure of **2**. Hydrogen atoms have been omitted for clarity.

In summary, both molecular structures are similar to those obtained for the analogous pentafluorophenyl derivatives previously described by us [5,6].

2.2. Computational Studies

Single point calculations on model systems of complexes **1** and **2** were performed at the Density Functional Theory (DFT) level of theory, using the PBE functional as implemented in TURBOMOLE 6.4 [16].

The bonding and conformational trends experimentally observed for complexes **1** and **2** were analyzed through a topological analysis of the DFT density, employing non-covalent interaction (NCI) calculations [17]. The NCI isosurfaces provide the non-covalent interactions as broad regions of density with a spatial distribution in real space. Since a quantitative assessment of the interaction energies cannot be achieved, a qualitative assessment of each type of non-covalent interaction, in terms of repulsion/attraction and strength (weak/medium/strong), can be obtained. For this, the electron density times the sign of the second Hessian eigenvalue ($\text{sign}(\lambda_2)\rho$) can be mapped on isosurfaces of the reduced density gradient $\sigma(r)$. If the sign of the λ_2 is positive, steric and repulsive contacts are assigned and the isosurfaces appear red; if λ_2 is close to zero, van der Waals weak interactions are expected and the color of the isosurface is green; finally, if the sign of λ_2 is negative, attractive non-covalent contacts are assigned and blue (strong interactions) or green-blue (medium strength interactions) isosurfaces appear.

The results displayed in Figure 3 show several interesting trends. For the model of compound **1**, a red isosurface is detected within the four-membered heterocycle, in agreement with the high cyclic tension of closely placed atoms. The most interesting feature of the NCI analysis is the presence of green isosurfaces between each 3,5-dichlorotrifluorophenyl-phenyl pair, indicating the presence of four stabilizing π - π interactions between aromatic groups surrounding the Au_2P_2 heterocycle, therefore compensating for the internal repulsion in the molecule (see Figure S13 in Supplementary Materials). A careful examination of the distances between the four pairs of perhalophenyl and phenyl interacting rings shows that the shortest distances appear between one of the F atoms in the *ortho* position of a 3,5-dichlorotrifluorophenyl ring and the centroid of the phenyl ring (between 3.24 and 3.37 Å), confirming the gauche conformation adopted by the interacting rings. In order to generalize this behavior, we have computed the same NCI analysis on a model system of the previously described complex $[\text{Au}_2(\text{C}_6\text{F}_5)_4(\mu\text{-PPh}_2)_2]$ [6] (see Figure S14 in Supplementary Materials). In this case, a very similar distribution of the non-covalent interactions to that of complex **1** is observed, suggesting that the pentafluorophenyl-phenyl π - π interactions that surround the Au_2P_2 heterocycle also compensate for the repulsion within the molecule.

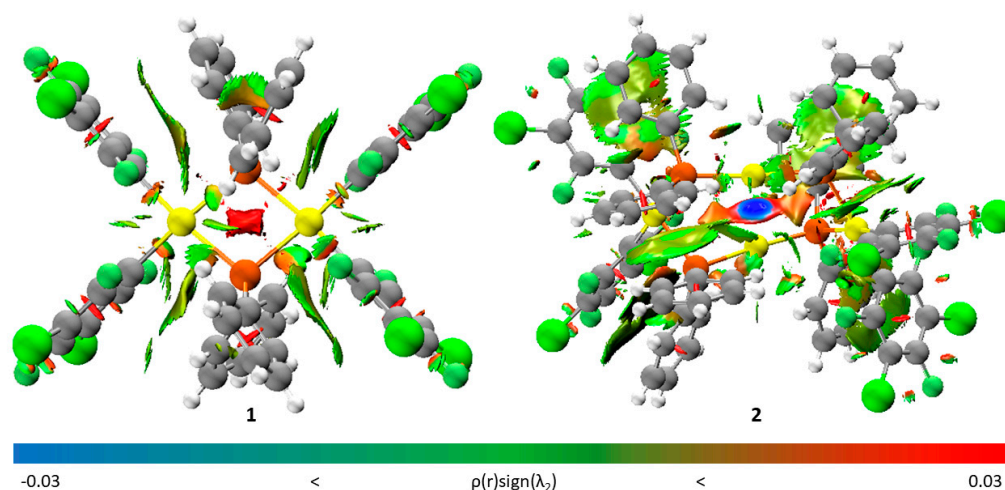


Figure 3. NCI-index isosurfaces from X-ray for **1** and **2** complexes. The isosurface value of s equals 0.5 a.u. and the electron density is such that $\rho \leq 0.015$ a.u. The scale for the relative magnitude of the interactions is presented at the bottom of the figure.

The π - π interactions between perhalophenyl groups and phenyl or heterocyclic groups have been previously reported [18–20]. This type of interaction, which is dispersive in nature, is also strengthened by an ionic contribution, since the outer part of the perhalophenyl rings is electron-rich because of the strong electron-withdrawing abilities of the halogen substituents that displace part of the aromatic electron density outwards from the ring; meanwhile, the outer part of the phenyl or heterocyclic groups is electron-poor because of the concentration of electron density in the aromatic ring. Therefore, an ionic component in the interaction increases its strength, compared to the usual aromatic π - π interactions. To account for this effect, we computed the electrostatic potential for complex **1**. Figure 4 depicts the electrostatic potential (ESP) isosurface for **1**, showing the commented electron-rich halogen substituents of the perhalophenyl groups and the electron-deficient H atoms in the phenyl ones.

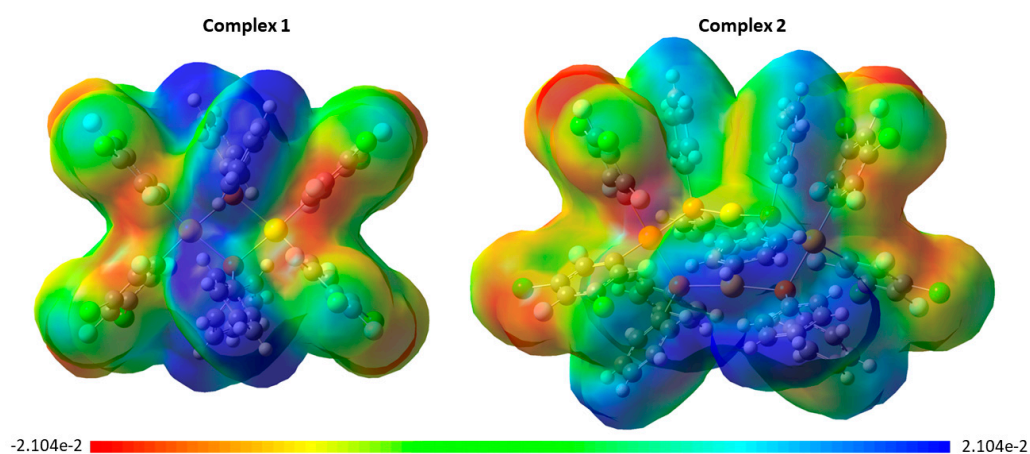


Figure 4. Electrostatic potential (ESP) mapped on the electron density (isoval = 0.0004) for complexes **1** and **2**.

The NCI analysis of a model of complex **2** also provides interesting conclusions (see Figure 3). First, the inclusion of Au(I) centers between phosphide bridging ligands provides an additional stabilization for the complex through the presence of a stabilizing auophilic interaction, represented in the real space as a blue isosurface and corresponding to a strong non-covalent interaction. In any case, the steric hindrance within the heterocycle is still reflected in this case, since orange-red isosurfaces around the auophilic interaction

appear, which are assigned to repulsions within the eight-membered ring. Again, the heterocycle is surrounded by π - π interactions between 3,5-dichlorotrifluorophenyl rings bonded to Au(III) and phenyl rings bonded to phosphorus in a gauche disposition but, in addition, π - π interactions between phenyl rings of different PPh_2^- units are observed, leading to a framework of π - π interactions around the complex core heterocycle. The above-mentioned ionic component of the perhalophenyl–phenyl interactions has also been computed and represented through an ESP isosurface, showing electron-rich regions in the halogen substituents of the perhalophenyl rings and electron-deficient H atoms in the phenyl ones.

Overall, the topological NCI and ESP analysis provides interesting insights into the stabilization of phosphanidogold(III) complexes bearing perhalophenyl ligands.

3. Materials and Methods

3.1. General

The starting materials $[\text{Au}_2(\text{C}_6\text{Cl}_2\text{F}_3)_2(\text{OEt}_2)_2]$ [21]; $[\text{NBu}_4][\text{Au}(\text{C}_6\text{Cl}_2\text{F}_3)_2\text{Cl}_2]$ and $[\text{NBu}_4][\text{Au}(\text{C}_6\text{Cl}_2\text{F}_3)_2]$ [22]; and $[\text{Au}_2(\text{C}_6\text{Cl}_2\text{F}_3)_4(\mu\text{-Cl})_2]$ [23] and $[\text{Au}(\text{tht})_2]\text{ClO}_4$ [24] were prepared following the synthetic procedures described in the references cited below. PPh_2H was acquired from Sigma-Aldrich and utilized as a 0.96 M tetrahydrofuran solution. All reactions were conducted under a dry N_2 atmosphere, employing standard Schlenk techniques. Solvents were procured from a solvent purification system (M-BRAUN MB SPS-800).

3.2. Materials and Physical Measurements

Conductivities were assessed in ca. 3×10^{-5} M acetone solutions using a Jenway 4010 conductimeter (Jenway, Felsted, UK). High-resolution mass spectrometry (HR-MS) data were acquired on a time-of-flight mass spectrometer equipped with an electrospray ionization (ESI) source (Bruker MicroTOF-Q spectrometer, Bruker Corporation, Bremen, Germany); accurate mass measurements were achieved through the utilization of sodium formate as an external reference. The analyses were carried out in negative and positive modes. Infrared spectra were acquired on a Nicolet Nexos FT-IR Spectrometer (Thermo Nicolet Corporation, Madison, WI, USA) covering the region from 4000 to 225 cm^{-1} , with Nujol mulls prepared between polyethylene sheets. $^{31}\text{P}\{^1\text{H}\}$, ^{20}F and ^1H NMR experiments were conducted on a Bruker AVANCE 400 (Bruker Corporation, Fällanden, Switzerland) in CDCl_3 solutions. Chemical shifts are reported in parts per million (ppm) and referenced to H_3PO_4 (^{31}P , external), CFCl_3 (^{19}F , external) and SiMe_4 (^1H , external). Multiplicities are denoted as singlet (s), broad singlet (br s) or multiplet (m). C, H and N analyses were carried out with a C.E. Instrument EA-1110 CHNSO microanalyzer (Carlo Erba, Milan, Italy).

3.3. Synthesis

3.3.1. Synthesis of $[\{\text{Au}(\text{C}_6\text{Cl}_2\text{F}_3)_2\}_2(\mu\text{-PPh}_2)_2]$ (1)

A freshly prepared 0.96 M solution of diphenylphosphine in tetrahydrofuran (THF) (0.208 mL, 0.2 mmol) was cautiously added to a solution of $[\text{Au}_2(\text{C}_6\text{Cl}_2\text{F}_3)_4(\mu\text{-Cl})_2]$ (0.1265 g, 0.1 mmol) in 20 mL of diethyl ether under a dry nitrogen atmosphere. The reaction mixture was vigorously stirred for 2 h at ambient temperature to facilitate the reaction, and, after this period of time, a white solid was formed. Subsequently, the resulting precipitate was isolated via filtration, washed three times with 3 mL portions of cold *n*-hexane each (3×1 mL) to remove any impurities and dried under vacuum. This process yielded the novel complex $[\{\text{Au}(\text{C}_6\text{Cl}_2\text{F}_3)_2\}_2(\mu\text{-PPh}_2)_2]$ (1) as a white solid (0.0751 g, 48%).

Anal. Calcd. (%) for $\text{C}_{48}\text{H}_{20}\text{Au}_2\text{Cl}_8\text{F}_{12}\text{P}_2$: C, 36.86; H, 1.29. Found: C, 36.80; H, 1.25. Λ_M (acetone): $6\ \Omega^{-1}\text{ cm}^2\text{ mol}^{-1}$. HR-MS (–): $m/z = 1594.7359$ Da, $[\text{Au}_2(\text{C}_6\text{Cl}_2\text{F}_3)_4(\mu\text{-PPh}_2)_2] + \text{Cl}^-$ (calculated $m/z = 1594.738223$ Da). FTIR (Nujol mulls): ν ($\text{Au}^{\text{III}}\text{-C}_6\text{Cl}_2\text{F}_3$) = 1593 (vs), 1055 (vs), 1136 (vs) and 779 cm^{-1} (vs). ^1H NMR (CDCl_3 , 298K), δ 7.52–7.38 ppm (m, 20H, Ph). ^{19}F NMR (CDCl_3 , 298K), δ –94.55 (s, 8F, *o*-F), –114.27 ppm (s, 4F, *p*-F). $^{31}\text{P}\{^1\text{H}\}$ NMR (CDCl_3 , 298K), δ –137.0 ppm (br s).

3.3.2. Synthesis of $[\{\text{Au}(\text{C}_6\text{Cl}_2\text{F}_3)_2(\mu\text{-PPh}_2)_2\text{Au}\}_2]$ (**2**)

To a solution of $[\text{NBu}_4][\text{Au}(\text{C}_6\text{Cl}_2\text{F}_3)_2\text{Cl}_2]$ (0.1820 g, 0.2 mmol) in 20 mL of diethyl ether under a nitrogen atmosphere, AgClO_4 (0.0829 g, 0.4 mmol) was added. The reaction mixture was stirred and shielded from direct light for 5 h to facilitate the reaction. Following this period, the white precipitate formed, identified as AgCl , was removed by filtration through celite under N_2 to obtain a clear solution. To the freshly prepared solution of $[\text{Au}(\text{C}_6\text{Cl}_2\text{F}_3)_2(\text{OEt}_2)_2]\text{ClO}_4$, $[\text{Au}(\text{tht})_2]\text{ClO}_4$ (0.0946 g, 0.2 mmol) was added, as well as a freshly prepared 0.96 M solution of PPh_2H in tetrahydrofuran (THF) (0.416 mL, 0.4 mmol). The resulting solution was stirred for 1 h, and, after this period of time, a white solid, $[\{\text{Au}(\text{C}_6\text{Cl}_2\text{F}_3)_2(\mu\text{-PPh}_2)_2\text{Au}\}_2]$ (**2**), appeared. The solid product was then filtered, washed with three fractions of 3 mL of cold *n*-hexane each (3×1 mL) to remove any impurities and dried under vacuum to yield the new complex (**2**) as a white solid (0.1865 g, 80%).

Anal. Calcd. (%) for $\text{C}_{72}\text{H}_{40}\text{Au}_4\text{Cl}_8\text{F}_{12}\text{P}_4$: C, 37.14; H, 1.73. Found: C, 37.31; H, 1.68. Λ_M (acetone): $54 \Omega^{-1} \text{cm}^2 \text{mol}^{-1}$. HR-MS (+): $m/z = 2346.8008$ Da, $[\{\text{Au}(\text{C}_6\text{Cl}_2\text{F}_3)_2(\mu\text{-PPh}_2)_2\text{Au}\}_2] + \text{Na}^+$ (calculated $m/z = 2346.795203$ Da). FTIR (Nujol mulls): ν ($\text{Au}^{\text{III}}\text{-C}_6\text{Cl}_2\text{F}_3$): 1593 (vs), 1055 (vs), 1134 (vs) and 779cm^{-1} (vs). ^1H NMR (CDCl_3 , 298K), δ 7.47–7.12 ppm (m, 40H, Ph). ^{19}F NMR (CDCl_3 , 298K), δ -94.77 (s, 8F, *o*-F), -116.50 ppm (s, 4F, *p*-F). $^{31}\text{P}\{^1\text{H}\}$ NMR (CDCl_3 , 298K), δ -35.62 ppm (br s).

3.4. Crystallography

Suitable single crystals were mounted in inert oil on a MiteGen MicroMount and transferred to the cold nitrogen stream of a Bruker APEX-II CCD area-detector diffractometer, equipped with an Oxford Instruments low-temperature controller system (Mo $K\alpha = 0.71073 \text{ \AA}$, graphite monochromator). Data were collected in ω - and ϕ -scan modes. Absorption effects were treated by numerical correction for crystal shape. The structures were elucidated using the olex2.solve 1.5 [25] structure solution program and refined on F_0^2 (SHELXL 2018/3) [26]. All non-hydrogen atoms were treated anisotropically, while all hydrogen atoms were included as riding bodies. A solvent mask consistent with 0.75 molecules per molecule of complex ($1 \cdot 0.75\text{CHCl}_3$) was applied. In the case of the crystal structure of complex **2**, although the nature of the complex, as well as the connectivity of the atoms, are perfectly clear, the min/max residual electron density peaks, located in the vicinity of the gold(I) atoms, as expected in structures containing heavy atoms, are unacceptably high to consider this structure publishable as it is. Although different crystals and absorption correction models have been employed, no good enough parameters have been obtained for this structure so as to publish the results. Table S1 contains crystallographic data and structure refinement details for compounds **1** and **2**. The supplementary crystallographic data for this paper can be found in CCDC-2156075. These data are accessible free of charge via www.ccdc.cam.ac.uk/conts/retrieving.html or by contacting The Cambridge Crystallographic Data Centre, 12 Union Road, Cambridge CB2 1EZ, UK; fax: +44 1223 336033.

3.5. Computational Details

The model systems of complexes **1** and **2** utilized in the theoretical studies were constructed based on the X-ray diffraction results and fully optimized at the Density Functional Theory (DFT) level employing the PBE functional [27,28], along with the corresponding dispersion correction of Grimme [29], as implemented in TURBOMOLE 6.4 [16]. A topological analysis of non-covalent interactions (NCI) for each model was conducted using the Multiwfn software [30]. The electron density representations were generated using the VMD software for visualizing the results [31]. The electron density from the total DFT density mapped with the electrostatic potential (ESP) was computed for model systems of complexes **1** and **2** using Gaussian16 and Gaussview 6.0 [32,33].

4. Conclusions

In conclusion, two novel and stable cyclic phosphide gold compounds, a gold(III) derivative and a mixed gold(I)/gold(III) complex, were synthesized and structurally characterized. The experimental and computational analyses carried out on these two new complexes indicated that the π - π interactions between 3,5-dichlorotrifluorophenyl and phenyl groups surrounding the four-membered or eight-membered ring heterocycles largely contribute to the stability of these systems. From these studies, we can also conclude that the high degree of repulsion found within the heterocycles in this type of derivative could be the reason for the low stability of other cyclic phosphide compounds.

Supplementary Materials: The following supporting information can be downloaded at <https://www.mdpi.com/article/10.3390/inorganics12030078/s1>, Figure S1: FT-IR spectrum of complex 1; Figure S2: FT-IR spectrum of complex 2; Figure S3: ^1H NMR spectrum of complex 1; Figure S4: ^1H NMR spectrum of complex 2; Figure S5: ^{19}F NMR spectrum of complex 1; Figure S6: ^{19}F NMR spectrum of complex 2; Figure S7: $^{31}\text{P}\{^1\text{H}\}$ NMR spectrum of complex 1; Figure S8: $^{31}\text{P}\{^1\text{H}\}$ NMR spectrum of complex 2; Figure S9: Simulated isotope pattern of $(\text{M} + \text{Cl})^-$ for compound 1; Figure S10: HR-MS (ESI-) for compound 1; Figure S11: Simulated isotope pattern of $(\text{M} + \text{Na})^+$ for compound 2; Figure S12: HR-MS (ESI+) for compound 2; Figure S13: Shortest F...centroid distances found for π - π interactions in 1; Figure S14: NCI-index isosurfaces from X-ray for $[\{\text{Au}(\text{C}_6\text{F}_5)_2\}_2(\mu\text{-PPh}_2)_2]$ complex; Table S1: Crystallographic data and structure refinement details for compounds 1 and 2.

Author Contributions: All authors contributed to the writing of the manuscript. Conceptualization, J.M.L.-d.-L., M.M. and M.E.O.; X-ray analysis, S.M. and M.E.O.; investigation, L.C.-G.; methodology, L.C.-G. and M.R.-C.; writing—original draft preparation, L.C.-G.; writing—review and editing, M.E.O.; supervision, J.M.L.-d.-L. and M.E.O.; project administration, J.M.L.-d.-L.; funding acquisition, J.M.L.-d.-L., M.M. and M.E.O. All authors have read and agreed to the published version of the manuscript.

Funding: This research was funded by the Spanish D.G.I. MINECO/FEDER (project number PID2022-139739NB-00I) AEI/FEDER, UE.

Data Availability Statement: Data are contained within the article and Supplementary Materials.

Acknowledgments: This research was supported by the Spanish D.G.I. MINECO/FEDER (project number PID2022-139739NB-00I, AEI/FEDER, UE). L.C.-G. acknowledges the University of La Rioja for her predoctoral grant.

Conflicts of Interest: The authors declare no conflicts of interest.

References

1. Dyson, D.B.; Parish, R.V.; McAuliffe, C.A.; Pritchard, R.G.; Fields, R.; Beagley, B. Gold(I) Complexes Derived from Secondary Phosphines: $[\{\text{Au}(\mu\text{-PR}_2)_n\}_n]$, $[(\text{AuBr})_2(\mu\text{-PPh}_2)]^-$, $[\text{AuX}(\text{PHR}_2)]$, and $[\{\text{Au}(\text{PHR}_2)\text{N}\}]^+$. Crystal Structure of $[\text{AuBr}(\text{PPhPh}_2)]$. *J. Chem. Soc. Dalton Trans.* **1989**, *5*, 907–914. [[CrossRef](#)]
2. Vicente, J.; Chicote, M.T.; Jones, P.G. (Diphenylphosphine)-, (Diphenylphosphido)-, and (Diphenylphosphinito)Gold(I) Complexes. Crystal Structure of $[(\text{PPh}_3)_2\text{N}][\text{Au}\{\text{P}(\text{O})\text{Ph}_2\}_2]$. *Inorg. Chem.* **1993**, *32*, 4960–4964. [[CrossRef](#)]
3. Puddephatt, R.J.; Thompson, P.J. Some Reactions of Methylplatinum and Methylgold Compounds with Phenylselenol, Diphenylphosphine, Diphenylarsine, N-Bromosuccinimide and 2-Nitrophenylsulphenyl Chloride. *J. Organomet. Chem.* **1976**, *117*, 395–403. [[CrossRef](#)]
4. Li, X.-S.; Mo, J.; Zhang, S.-M.; Yuan, L.; Liu, J.-H. $(\mu\text{-Diphenylphosphanido-K}^2\text{P:P}')$ bis [2,2'-(pyridine-2,6-diyl)diphenyl- $\text{K}^3\text{C}^1, \text{N}, \text{C}^1'$]Gold(III)] Perchlorate Acetonitrile Solvate. *Acta Crystallogr. Sect. E Struct. Rep. Online* **2008**, *64*, m1126–m1127. [[CrossRef](#)]
5. Blanco, M.C.; Fernández, E.J.; López-de-Luzuriaga, J.M.; Olmos, M.E.; Crespo, O.; Gimeno, M.C.; Laguna, A.; Jones, P.G. Heteropolynuclear Phosphide Complexes: Phosphorus as Unique Atom Bridging Coinage Metal Centres. *Chem. Eur. J.* **2000**, *6*, 4116–4123. [[CrossRef](#)] [[PubMed](#)]
6. Blanco, M.C.; Fernández, E.J.; Fischer, A.K.; Jones, P.G.; Laguna, A.; Olmos, M.E.; Villacampa, M.D. $\text{NBu}_4[\{\text{Au}(\text{C}_6\text{F}_5)_3\}_2(\text{m-PPh}_2)]$: A Gold(III) Phosphide with a Single Bridging the Metallic Centers. *Inorg. Chem. Commun.* **2000**, *3*, 163–165. [[CrossRef](#)]
7. Coconubo-Guio, L.; López-de-Luzuriaga, J.M.; Moreno, S.; Olmos, M.E. Synthesis and Structural Characterization of Phosphide Gold(III)/Gold(I) Complexes and Their Thallium(III) and Gold(III) Precursors. *Molecules* **2023**, *28*, 447. [[CrossRef](#)] [[PubMed](#)]

8. Weber, L.; Lassahn, U.; Stammler, H.-G.; Neumann, B.; Karaghiosoff, K. Synthesis and Structure of the Decanuclear Gold(I) Cluster Cation $[\text{Au}_8(\text{AuCl})_2\{\mu_3\text{-P}(\text{Tbu})\}_2\{\mu\text{-P}(\text{Tbu})=\text{C}(\text{NMe}_2)_2\}_6]^{4+}$ with Bridging Phosphaalkene and Phosphanediide Ligands. *Eur. J. Inorg. Chem.* **2002**, *2002*, 3272–3277. [[CrossRef](#)]
9. Azizpoor Fard, M.; Rabiee Kenaree, A.; Boyle, P.D.; Ragogna, P.J.; Gilroy, J.B.; Corrigan, J.F. Coinage Metal Coordination Chemistry of Stable Primary, Secondary and Tertiary Ferrocenylethyl-Based Phosphines. *Dalton Trans.* **2016**, *45*, 2868–2880. [[CrossRef](#)] [[PubMed](#)]
10. Paderina, A.V.; Koshevoy, I.O.; Grachova, E.V. Keep It Tight: A Crucial Role of Bridging Phosphine Ligands in the Design and Optical Properties of Multinuclear Coinage Metal Complexes. *Dalton Trans.* **2021**, *50*, 6003–6033. [[CrossRef](#)] [[PubMed](#)]
11. Fernández, E.; Laguna, A.; Olmos, M.E. Perfluoroarylgold Complexes. *Coord. Chem. Rev.* **2008**, *252*, 1630–1667. [[CrossRef](#)]
12. Mastrorilli, P.; Fortuño, C. Platinum and Palladium Promoted Couplings of Bridging PPh_2 -with Terminally Bonded Ligands. *Inorganica Chim. Acta* **2020**, *513*, 119947. [[CrossRef](#)]
13. Ara, I.; Forniés, J.; Ibáñez, S.; Mastrorilli, P.; Todisco, S.; Gallo, V. Polynuclear Platinum Phosphanido/Phosphinito Complexes: Formation of P–O and P–O–P Bonds through Reductive Coupling Processes. *Dalton Trans.* **2016**, 2156–2171. [[CrossRef](#)] [[PubMed](#)]
14. Álvarez, S. A cartography of the van der Waals territories. *Dalton Trans.* **2013**, *42*, 8617–8636. [[CrossRef](#)] [[PubMed](#)]
15. Hu, S.Z.; Zhou, Z.H.; Xie, Z.X.; Robertson, B.E. A comparative study of crystallographic van der Waals radii. *Z. Krist. Mater.* **2014**, *229*, 517–523. [[CrossRef](#)]
16. Ahlrichs, R.; Bär, M.; Häser, M.; Horn, H.; Kölmel, C. Electronic Structure Calculations on Workstation Computers: The Program System Turbomole. *Chem. Phys. Lett.* **1989**, *162*, 165–169. [[CrossRef](#)]
17. Johnson, E.R.; Keinan, S.; Mori-Sánchez, P.; Contreras-García, J.; Cohen, A.J.; Yang, W. Revealing Noncovalent Interactions. *J. Am. Chem. Soc.* **2010**, *132*, 6498–6506. [[CrossRef](#)] [[PubMed](#)]
18. Vangala, V.R.; Nangia, A.; Lynch, V.M. Interplay of Phenyl–Perfluorophenyl Stacking, C–H \cdots F, C–F \cdots π and F \cdots F Interactions in Some Crystalline Aromatic Azines. *Chem. Commun.* **2002**, *12*, 1304–1305. [[CrossRef](#)]
19. Sonoda, Y.; Goto, M.; Tsuzuki, S.; Tamaoki, N. Fluorinated Diphenylpolyenes: Crystal Structures and Emission Properties. *J. Phys. Chem. A* **2007**, *111*, 13441–13451. [[CrossRef](#)]
20. Echeverría, R.; López-de-Luzuriaga, J.M.; Monge, M.; Moreno, S.; Olmos, M.E.; Rodríguez-Castillo, M. Lead Encapsulation by a Golden Clamp through Multiple Electrostatic, Metallophilic, Hydrogen Bonding and Weak Interactions. *Chem. Commun.* **2018**, *54*, 295–298. [[CrossRef](#)]
21. Laguna, A.; Laguna, M.; Jiménez, J.; Fumanal, A.J. 2,4,6-Trifluorophenyl Gold(I) and Gold(III) Complexes. *J. Organomet. Chem.* **1990**, *396*, 121–128. [[CrossRef](#)]
22. Uson, R.; Laguna, A.; Garcia, J.; Laguna, M. Anionic Perfluorophenyl Complexes of Gold(I) and Gold(III). *Inorganica Chim. Acta* **1979**, *37*, 201–207. [[CrossRef](#)]
23. Usón, R.; Laguna, A.; Laguna, M.; Abad, M. Synthesis and Reactions of Di- μ -Halo- or -Pseudohalotetrakis(Pentafluorophenyl) Digold(III). *J. Organomet. Chem.* **1983**, *249*, 437–443. [[CrossRef](#)]
24. Usón, R.; Laguna, A.; Navarro, A.; Parish, R.V.; Moore, L.S. Synthesis and Reactivity of Perchlorate Bis(Tetrahydrothiophen)Gold(I). 197Au Mössbauer Spectra of Three-Coordinate Gold(I) Complexes. *Inorganica Chim. Acta* **1986**, *112*, 205–208. [[CrossRef](#)]
25. Bourhis, L.J.; Dolomanov, O.V.; Gildea, R.J.; Howard, J.A.K.; Puschmann, H. The Anatomy of a Comprehensive Constrained, Restrained Refinement Program for the Modern Computing Environment—Olex2 Dissected. *Acta Crystallogr. A Found. Adv.* **2015**, *71*, 59–75. [[CrossRef](#)] [[PubMed](#)]
26. Sheldrick, G.M. SHELXT—Integrated Space-Group and Crystal-Structure Determination. *Acta Crystallogr. A Found. Adv.* **2015**, *71*, 3–8. [[CrossRef](#)]
27. Parr, R.G.; Yang, W. *Density-Functional Theory of Atoms and Molecules*; Oxford University Press: New York, NY, USA, 1989.
28. Lee, C.; Yang, W.; Parr, R.G. Development of the Colle-Salvetti Correlation-Energy Formula into a Functional of the Electron Density. *Phys. Rev. B* **1988**, *37*, 785–789. [[CrossRef](#)]
29. Grimme, S.; Antony, J.; Ehrlich, S.; Krieg, H. A Consistent and Accurate Ab Initio Parametrization of Density Functional Dispersion Correction (DFT-D) for the 94 Elements H–Pu. *J. Chem. Phys.* **2010**, *132*, 154104. [[CrossRef](#)]
30. Lu, T.; Chen, F. Multiwfn: A Multifunctional Wavefunction Analyzer. *J. Comput. Chem.* **2012**, *33*, 580–592. [[CrossRef](#)]
31. Humphrey, W.; Dalke, A.; Schulten, K. VMD: Visual Molecular Dynamics. *J. Mol. Graph.* **1996**, *14*, 33–38. [[CrossRef](#)] [[PubMed](#)]
32. *Gaussian 16, Revision C.01*, Frisch, M.J., Trucks, G.W., Schlegel, H.B., Scuseria, G.E., Robb, M.A., Cheeseman, J.R., Scalmani, G., Barone, V., Petersson, G.A., Nakatsuji, H.; et al., Eds.; Gaussian, Inc.: Wallingford, CT, USA, 2016.
33. *GaussView, Version 6*, Dennington, R., Keith, T.A., Millam, J.M., Eds.; Semichem Inc.: Shawnee Mission, KS, USA, 2016.

Disclaimer/Publisher’s Note: The statements, opinions and data contained in all publications are solely those of the individual author(s) and contributor(s) and not of MDPI and/or the editor(s). MDPI and/or the editor(s) disclaim responsibility for any injury to people or property resulting from any ideas, methods, instructions or products referred to in the content.